

# Closely Spaced Miniaturized MIMO Antenna for X and Ku Band Applications Using Metamaterial

Jyothsna Undrakonda\* and Ratna Kumari Upadhyayula

*Department of EECE, GITAM Deemed to be University, Visakhapatnam, A.P, India*

**ABSTRACT:** The design of a low profile rectangular patch multi-input multi-output (MIMO) antenna is proposed. The antenna incorporates a novel metamaterial-based structure and utilizes a three single split ring resonators based tank circuit to achieve high isolation. A novel metastructure covers C, X, and Ku bands. The antenna structure is made up three single split ring resonators (SRRs) embedded on the bottom of the antenna, situated between the radiating patches. The dimensions of the fabricated antenna are  $10 \times 15 \times 1.6 \text{ mm}^3$  on an FR4 epoxy substrate. The antenna operates within the frequency range of 10.97 to 18.85 GHz with minimum spacing between antenna elements as 2 mm, covering the X and Ku bands. It is utilized in radar and satellite applications. The metastructure on the back of the antenna enhances isolation by more than 16 dB in the operating band, with a maximum of  $-31.28 \text{ dB}$  at 17.88 GHz. The antenna's radiation efficiency and gain are increased by 80% and 5.54 dB at a frequency of 16.37 GHz respectively. The antenna exhibits good diversity performance parameters, such as an ECC below 0.1 and a DG of 9.98 dB, in addition to desirable radiation characteristics. The proposed antenna exhibits the features that make it highly suitable for advanced technologies.

## 1. INTRODUCTION

In the field of communication systems, there is a constant requirement for novel approaches to enhance data rates while minimize channel losses. The design of the antenna is crucial for achieving the requirements of emerging technologies. In order to achieve the necessary operating frequency range with desirable characteristics, and it is important for the antenna design to be small in size. MIMO wireless technology fulfils the requirements for modern high-data-rate communication systems by providing enhanced data rates, system performance, and dependability. It is vital for designing a compact MIMO antenna that has excellent isolation. Several decoupling approaches have been suggested in the literature to enhance the separation between antenna elements. A potential method to achieve effective isolation in MIMO antennas is by using a MIMO design based on metamaterials [1–3]. A metasurface that consists of square split-ring resonators (SRRs) is placed on the antenna array to enhance decoupling [4, 5]. The decoupling structure [6] is designed using a split ring that includes an inductive line and a capacitive gap. The inductive line enables magnetic coupling, while the capacitive gap facilitates electrical coupling. The mentioned strategies comprise slots and meandering lines [7], orthogonal feeding [8], diversity techniques [9], EBG structure [10], and band stop filters [11, 12]. The antenna utilized a metasurface to function in three frequency bands, namely X, Ku, and K. It obtained an impressive isolation level of 32 dB, as reported in [13]. A metasurface is utilized to achieve various operating frequencies covering S- and X-band frequencies [14]. The EBG structure is designed with metamaterial to efficiently isolate the Ultra-Wideband (UWB) antenna from 8 to 40 GHz,

resulting in an excellent isolation of 37 dB [15]. Single Negative Metamaterial (SNG) is employed as a decoupling component for UWB applications [16]. To mitigate reciprocal coupling, decoupling slabs and metasurface-based slots are utilized [17, 18]. A metamaterial based EBG is used to enhance the isolation, as described in [19].

Although the above-mentioned works are afflicted by low bandwidth and increased dimensions when being employed for particular frequency band applications, the metastructure technique offers a broader range of decoupling capabilities than alternative decoupling methods. Nevertheless, it has limits with regard to of bandwidth and depends on a rigid design model.

This article presents a novel metastructure unit cell to be utilized as a decoupling element. Three circular split ring resonators are incorporated as tank networks at the base of the antenna to enhance the isolation between the multiple-input multiple-output (MIMO) antenna elements within a small size. The proposed decoupling work distinguishes itself from other decoupling schemes and has the following impacts:

- The antenna's miniaturization has been achieved by utilizing a metamaterial structure, while maintaining good performance parameters.
- The spacing among radiating elements is very small, leading to mutual coupling effect. The issue is effectively resolved through the use of a novel metamaterial structure.
- The compact MIMO antenna employs rectangular patches with a 3 single split-ring resonators based tank circuit to achieve effective isolation over a wide operating band. The ease of its nature makes it easy to design and fabricate.

\* Corresponding author: Jyothsna Undrakonda (jyothsna.1511@gmail.com).

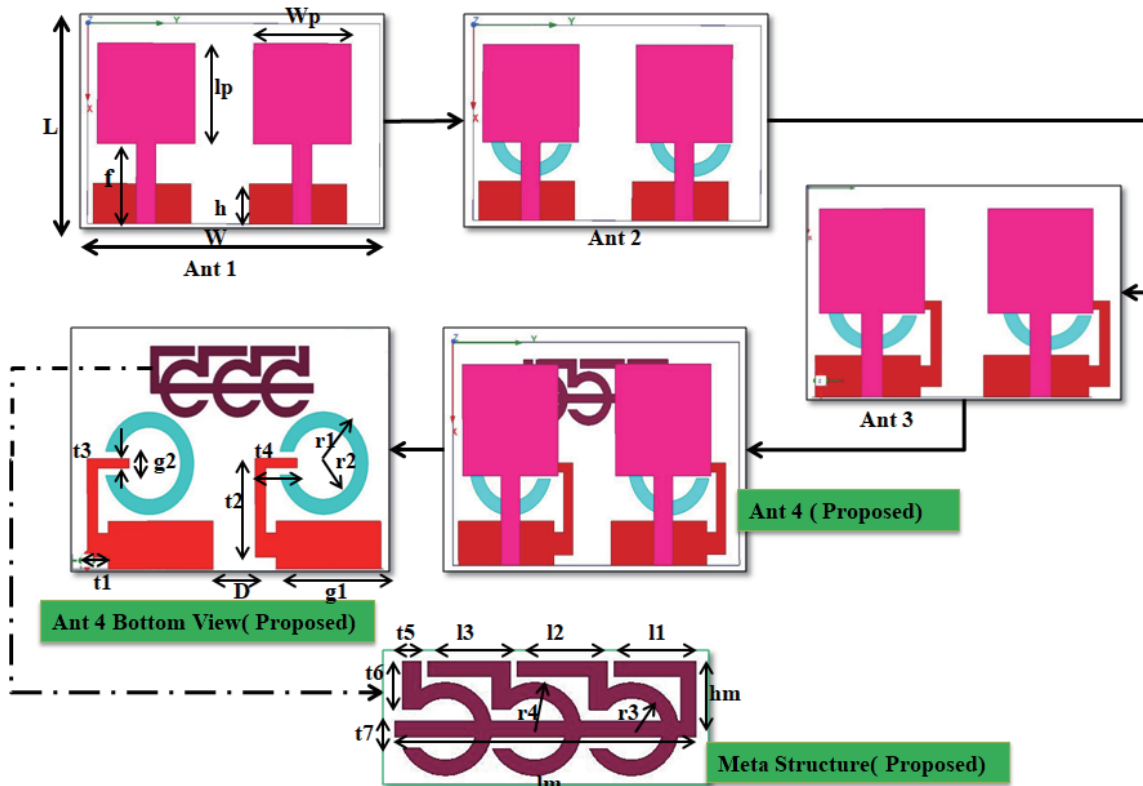


FIGURE 1. MIMO antenna design evaluation steps.

- The proposed antenna's novelty lies in its decoupling element, consisting of three single SRRs connected in series. This configuration forms LC networks that significantly affect the operating band and isolation. Higher bands with good isolation can be achieved.
- The decoupling tank circuit has multiple applications that can be achieved by adjusting the characteristic parameter of the decoupling element, such as the radius. The change in the inductance and capacitance of its design enhances the performance of the antenna.
- The variability of radiation patterns at operational frequencies allows for increased data transfer rates.

The proposed compact MIMO antenna, incorporating a three-SRR based tank circuit, is well suited for wide-band applications and exhibits good isolation.

## 2. METHODOLOGY TO DESIGN ANTENNA AND META STRUCTURE

### 2.1. Theoretical Analysis of Antenna and Decoupling Element

The MIMO antenna consists of a rectangular patch with a tank-type metastructure formed by three split ring resonators, as shown in Figure 1. This antenna is referred to as Ant 4. The antenna's ground component has been altered using a meta structure.

It is connected to a rectangular ground with a tank circuit, which includes a split ring. This setup is represented as Ant 4 in the bottom view of Figure 1. The dimensions (in 'mm') of the MIMO antenna are  $L = 10$ ,  $W = 15$ ,  $lp = 5$ ,  $wp = 5$ ,  $f = 4$ ,  $h = 2$ ,  $r1 = 2.12$ ,  $r2 = 1.5$ ,  $g1 = 5$ ,  $g2 = 1$ ,  $D = 2$ ,  $t1 = 1$ ,  $t2 = 4.1$ ,  $t3 = 0.5$ ,  $t4 = 2$ ,  $t5 = 0.5$ ,  $t6 = 1.25$ ,  $t7 = 0.4$ ,  $hm = 1.95$ ,  $lm = 7.7$ ,  $l1 = l3 = 2.1$ ,  $l2 = 3.2$ .

The MIMO antenna proposed in this study has compact dimensions and a small spacing between the antenna elements, resulting in a significant mutual coupling effect. To mitigate the coupling impact, a metastructure featuring three unique split rings interconnected as a tank circuit can be utilized. The addition of a metamaterial at the bottom of an antenna affects the radiation effect between antenna elements due to the combined inductive and capacitive nature. The unit cell comprises the three tank circuits illustrated in Figure 2(c). The admittance of the metamaterial affects the operating band and isolation of the rectangular MIMO antenna.

To achieve impedance matching and maintain adequate isolation, it is required to appropriately link the decoupling circuit design on the bottom of the antenna with the parallel combination tank circuit consisting of L and C components of patches. The equations represent the mutual admittance of the equivalent circuit for each separate tank circuit of the antenna. The overall admittance of metastructure is shown in Figure 2(c),

$$Y = \frac{L_m Y_m}{L_m + Y_m} \quad (1)$$

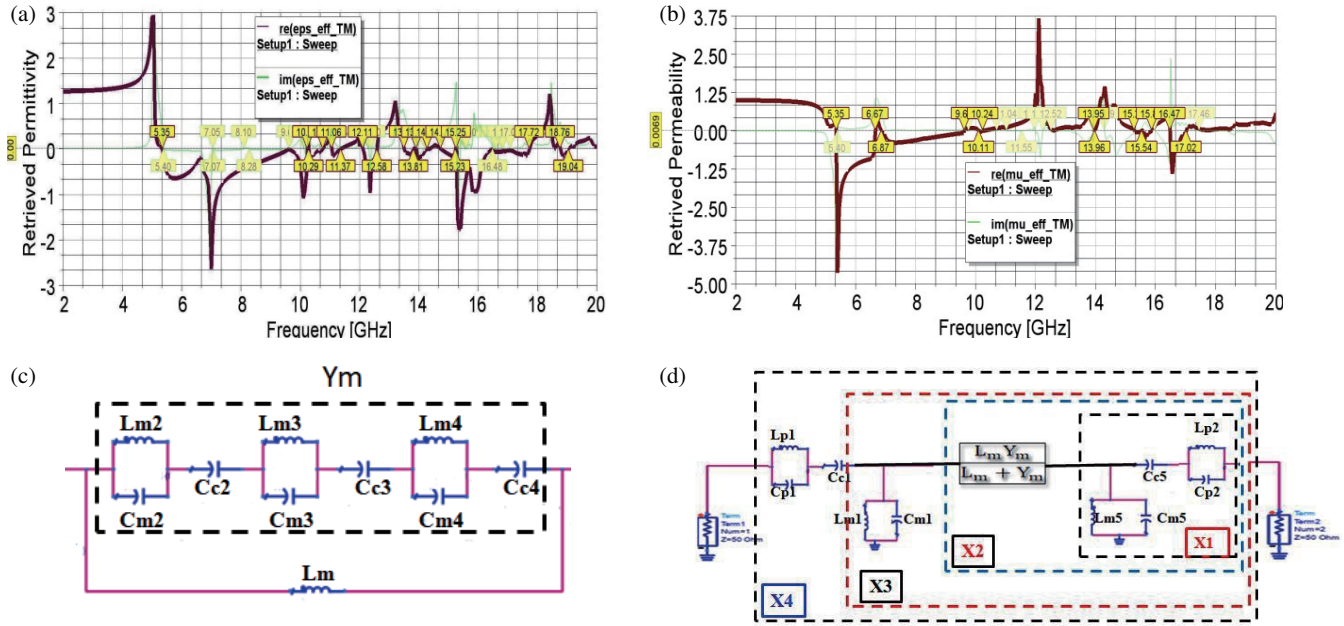


**FIGURE 2.** Characteristics of decoupling unit cell. (a) Permittivity. (b) Permeability. (c) Equivalent circuit of metastructure and (d) Overall equivalent circuit of proposed MIMO antenna.

The admittance of remaining networks shown in Figure 2(d) resolved as below,

$$X_1 = \frac{\left[ \frac{SC_{p2}}{1+S^2C_{p2}L_{p2}} - SC_{c5} \right] \left[ \frac{SC_{m5}}{1+S^2C_{m5}L_{m5}} \right]}{\left[ \frac{SC_{p2}}{1+S^2C_{p2}L_{p2}} - SC_{c5} \right] + \left[ \frac{SC_{m5}}{1+S^2C_{m5}L_{m5}} \right]} \quad (2)$$

$$X_2 = \frac{X_1 * \frac{L_m Y_m}{L_m + Y_m}}{X_1 + \frac{L_m Y_m}{L_m + Y_m}} \quad (3)$$

$$X_3 = \frac{X_2 * \frac{SC_{m1}}{1+S^2C_{m1}L_{m1}}}{X_2 + \frac{SC_{m1}}{1+S^2C_{m1}L_{m1}}} \quad (4)$$

$$X_4 = X_3 * SC_{c3} \frac{SC_{p1}}{1+S^2C_{p1}L_{p1}} \quad (5)$$

The operating frequency can be modified by appropriately tuning the parallel combination of  $L_{p1}$  and  $C_{p1}$ , as well as another tank circuit consisting of the parallel combination of  $L_{p2}$  and  $C_{p2}$ . The isolation of the proposed MIMO antenna is achieved by adjusting the values of  $L_{m1}$ ,  $L_{m2}$ ,  $L_{m3}$ ,  $L_{m4}$ ,  $L_{m5}$ ,  $C_{m1}$ ,  $C_{m2}$ ,  $C_{m3}$ ,  $C_{m4}$ , and  $C_{m5}$  of the three split ring resonator based tank circuit. The  $C_c$  capacitor serves as a coupling element between the ring connections and the coupling connection between the ground network and the rectangular patches. The optimum values of the equivalent circuit are estimated using Keysight ADS. As,  $L_{p1} = 0.2186$  nH,  $L_{p2} = 0.01$  nH,  $C_{p1} = 20$  pF,  $C_{p2} = 3.907$  pF,  $L_{m1} = 1$  nH,  $L_{m2} = 0.5$  nH,  $L_{m3} = 1.02$  nH,  $L_{m4} = 0.01$  nH,  $L_{m5} = 11.665$  nH,  $C_{m1} = 0.5$  pF,  $C_{m2} = 1.075$  pF,  $C_{m3} = 1.29$  pF,  $C_{m4} = 0.8$  pF,

$C_{m5} = 0.5$  pF,  $C_{c1} = 0.7595$  pF,  $C_{c2} = 1.31$  pF,  $C_{c3} = 0.8$  pF,  $C_{c4} = 1.09$  pF and  $C_{c5} = 1.45$  pF.

The resonance frequency of the analogous circuit was calculated by feeding the values of L and C into the equations. This frequency is within the specified range of frequencies that the antenna is designed to operate with. The S-parameters acquired from the ADS software are compared with the simulation parameters. The analysis concluded that the proposed antenna, when being combined with its decoupling network, effectively satisfies the criteria for wide band coverage and exhibits excellent isolation.

## 2.2. Metamaterial Design

The tank type metastructure is constructed with three compact single split ring resonators, where the ring radius of  $r_3$  is 1.2 mm, and the ring radius of  $r_4$  is 0.8 mm. The metastructure is simulated using the Floquet port and periodic boundary conditions in Ansys HFSS [3]. Figure 2 denotes the properties of permittivity, permeability, and index for the proposed metamaterial.

The proposed structure had epsilon negative behavior in the frequency range of 5.35 GHz to 10.2 GHz, 12.11 GHz to 10.29 GHz, 15.23 GHz to 17.72 GHz, and 18.76 GHz to 19.04 GHz. Additionally, it exhibited mu negative behavior in the frequency range of 5.35 GHz to 6.67 GHz, 6.84 GHz to 10.49 GHz, and 16.47 GHz to 17.03 GHz. The index ( $n$ ) is expressed as negative values inside the frequency ranges of 5.38 to 10.23 GHz, 13.92 to 14.28 GHz, 15.28 to 15.90 GHz, and 16.48 to 17.10 GHz. Through the investigation of the features of three single SRR based tank metastructure, it was

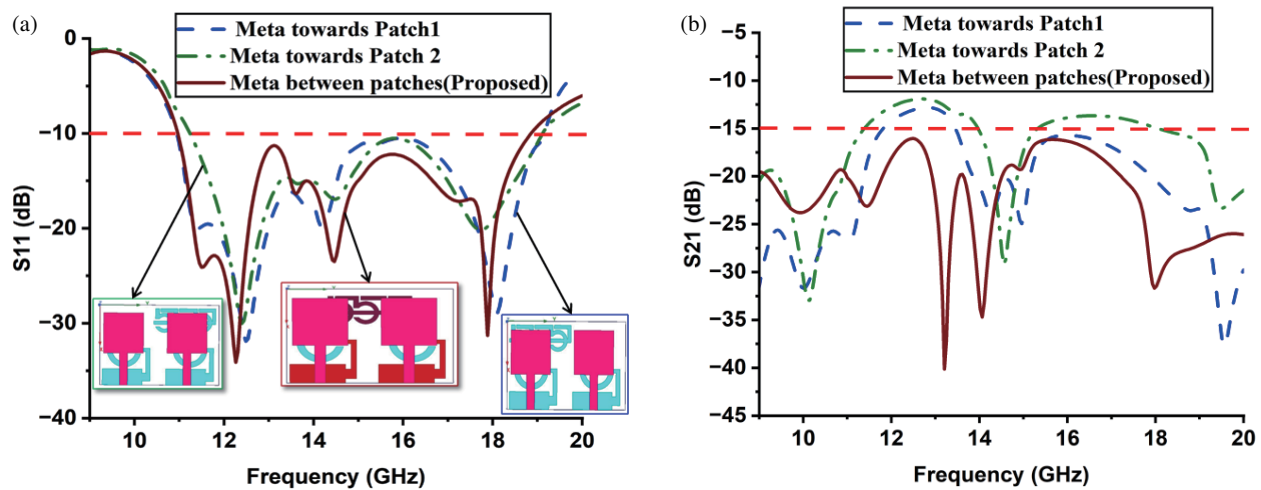


FIGURE 3.  $S$ -parameter variation with decoupling element optimetrics, (a)  $S_{11}$  and (b)  $S_{21}$ .

TABLE 1. Optimetrics analysis of decoupling structure.

| S. No | Optimetrics Condition           | Operating Band (GHz) | Isolation (dB) |
|-------|---------------------------------|----------------------|----------------|
| 1.    | Meta towards Patch 1            | 10.95–19.14 GHz      | < –13 dB       |
| 2.    | Meta between patches (Proposed) | 10.97–18.83 GHz      | < –16 dB       |
| 3.    | Meta towards Patch 2            | 11.27–19.10 GHz      | < –12 dB       |

determined that the metastructure operated in the C, X, and Ku bands.

### 2.3. Optimetrics of Metastructure

The proposed compact MIMO antenna effectively achieved a wide bandwidth and good isolation by utilizing a metamaterial structure. Three unique single-series-resonant (SRR) tank circuits are interconnected to form a metastructure, resulting in significant alterations in the  $S$ -parameters. Metastructure optimetrics analysis involves changing the placement of the metastructure on the ground plane of the antenna.

The unit cell was first positioned near patch 1, resulting in the observation of a broad frequency range spanning from 10.95 to 19.14 GHz, with an isolation level below –13 dB. The unit cell is strategically placed between radiating elements to redirect the field distribution, resulting in enhanced isolation for the proposed antenna. In this specific case of meta across patches, the realized operating band spans from 10.97 to 18.83 GHz. The isolation is more than 16 dB over the entire band and remains above 20 dB at frequencies ranging from 10.97 to 11.76 GHz, 12.93 to 14.5 GHz, and 17.20 to 20 GHz.

The meta cell is now located near patch 2 of the MIMO antenna. It is found to operate from 11.27 GHz to 19.1 GHz, with an isolation level above 12 dB. After analyzing the optimum position of the metastructure, it is clear that placing the meta unit cell at the bottom of the antenna, specifically at the centre of the two patches, leads to a favorable frequency band. This

arrangement achieves good isolation, with a maximum value of –31.2 dB at 17.88 GHz.

Figure 3 illustrates the variation of the  $S$ -parameters, such as  $S_{11}$  and  $S_{21}$ . Table 1 provides a concise overview of the changes in isolation and operating band caused by the position of the unit cell.

## 3. PROPOSED MIMO ANTENNA DESIGN EVOLUTION STEPS

The proposed antenna designed with a simple metamaterial structure. It has a circular form and is constructed using a substrate made of FR4 Epoxy with a relative permittivity ( $\epsilon_r$ ) of 4.4. The evolution of MIMO antenna involves four distinct steps, as depicted in Figure 1. Each change results in a noticeable alteration in the operating band and the mutual coupling between the individual antenna elements.

Initially, a rectangular patch antenna was built with small dimensions and a minimum spacing of 3 mm between antenna elements. The antenna's design successfully achieved dual operating bands covering from 11.04 GHz to 13.43 GHz and 16.71 GHz to 19.42 GHz. The level of isolation is measured to be –10 dB at two specific frequency ranges.

To enhance the antenna's performance in terms of isolation and impedance matching, a modification is made to the ground by adding a single circular split ring near the ground plane on the bottom of the antenna, as represented in Figure 1, labeled as Ant 2. This operation of the antenna results in dual bands span-

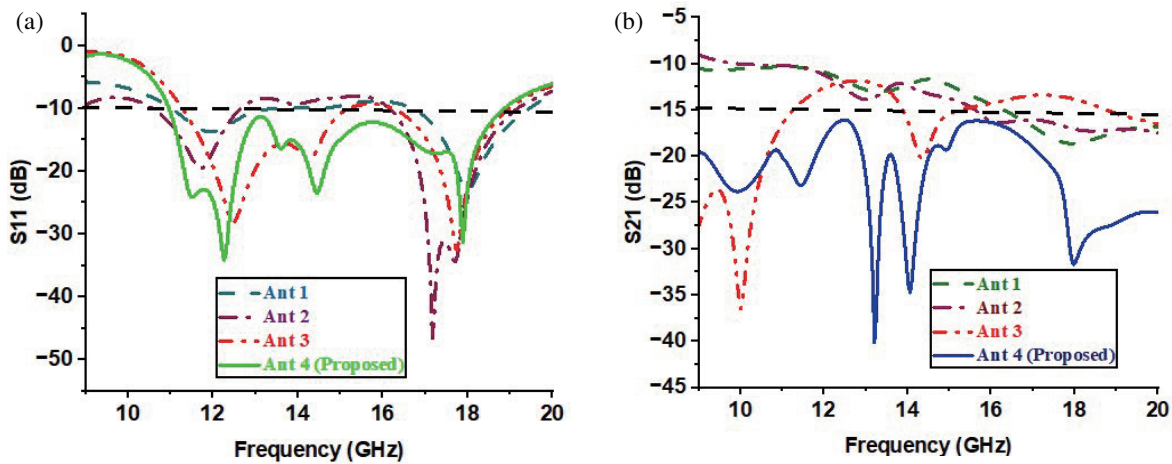


FIGURE 4.  $S$  parameters variation with antenna design modifications. (a)  $S_{11}$ , (b)  $S_{21}$ .

TABLE 2. Parameters analysis for antenna design evolution.

| S. No | Antenna Design   | Operating Band (GHz)              | Isolation |
|-------|------------------|-----------------------------------|-----------|
| 1.    | Ant 1            | 11.04–13.43 GHz & 16.71–19.42 GHz | < -10 dB  |
| 2.    | Ant 2            | 10.59–12.62 GHz & 16.17–19.14 GHz | < -10 dB  |
| 3.    | Ant 3            | 11.31–15.18 GHz & 16.26–18.96 GHz | < -12 dB  |
| 4.    | Ant 4 (Proposed) | 10.97–18.85 GHz                   | < -16 dB  |

ning from 10.59 to 12.62 GHz and 16.17 to 19.14 GHz, with an isolation level below  $-10$  dB. There still exists a need to improve the isolation and impedance matching in order to achieve high-speed data transfer.

Additionally, it is essential to enhance the isolation of the MIMO antenna, and the ground structure is altered by merging the rectangular ground and circular split ring to create a tank-like connection. Ant 3 modification operates within the frequency ranges of 11.34 GHz to 15.185 GHz and 16.265 GHz to 18.965 GHz, with an isolation level of  $-12$  dB. Using the antenna in such a way is also ineffective. The spacing between the radiating parts is a paltry 2 mm, resulting in a significant impact on the mutual coupling effect. To address this issue, the concept of metamaterial is proposed, which effectively improves the isolation and bandwidth of the antenna.

In this ultimate transformation, three single SRRs are linked in a sequential manner with a minimal separation of 1 mm, forming a tank circuit. This circuit is positioned at the bottom of the antenna, between its elements. Ant 4, a modified antenna, successfully accomplished a wide frequency range from 10.97 GHz to 18.85 GHz, covering the upper X band and Ku band. It also exhibited an isolation level of over 16 dB.

Figure 5 clearly demonstrates the variations of surface current distribution with the decoupling element for frequencies of 11.54 GHz, 12.26 GHz, 13 GHz, and 17.28 GHz. The metamaterial functions as a reflector for the radiation fields between antenna elements by varying its inductance and capacitance (LC network), as represented in Figure 2.

Figure 4 displays the  $S$ -parameter variations of four MIMO evolution models. The proposed antenna, equipped with

metamaterial, exhibits a maximum return loss of  $-34.11$  dB at 12.26 GHz,  $-23.49$  dB at 14.46 GHz, and  $-31.28$  dB at 17.88 GHz. The incorporation of metastructure has also altered isolation. The highest level of isolation reached was  $-31.28$  dB at 17.88 GHz. Table 2 provides the operating bands and isolation of each step of the proposed antenna. Ant 4 has been proposed, including minimal distance between them and excellent isolation.

## 4. RESULTS AND DISCUSSION

The proposed MIMO system consists of a circular patch antenna with three single split-ring resonators (SRRs) used as a decoupling circuit. The system is made using the S63LPKF Prototype machine. The performance characteristics were observed using the N9916A Keysight Field fox vector network analyzer. Figure 6(a) displays the variation of  $S$ -parameters with both simulated and measured antenna results. The operating frequency range of the manufactured antenna spans from 11.27 GHz to 18.96 GHz, encompassing the upper regions of the X-band and Ku-band. The isolation demonstrated excellent agreement with the simulated values. Specifically, it remained below  $-16$  dB across the entire operating frequency range. It reached a maximum value of  $-20.63$  dB at 14.46 GHz and  $-31.2$  dB at 17.88 GHz.

The MIMO antenna achieved an adequate omnidirectional pattern at frequencies of 12.12 GHz, 15.5 GHz, and 16.06 GHz by utilizing a design that incorporates a rectangular patch and three single SRRs based on metastructure. Figure 6(e) displays the  $E$ -plane and  $H$ -plane perspectives of co and cross polarization. The proposed MIMO antenna achieves an efficiency of

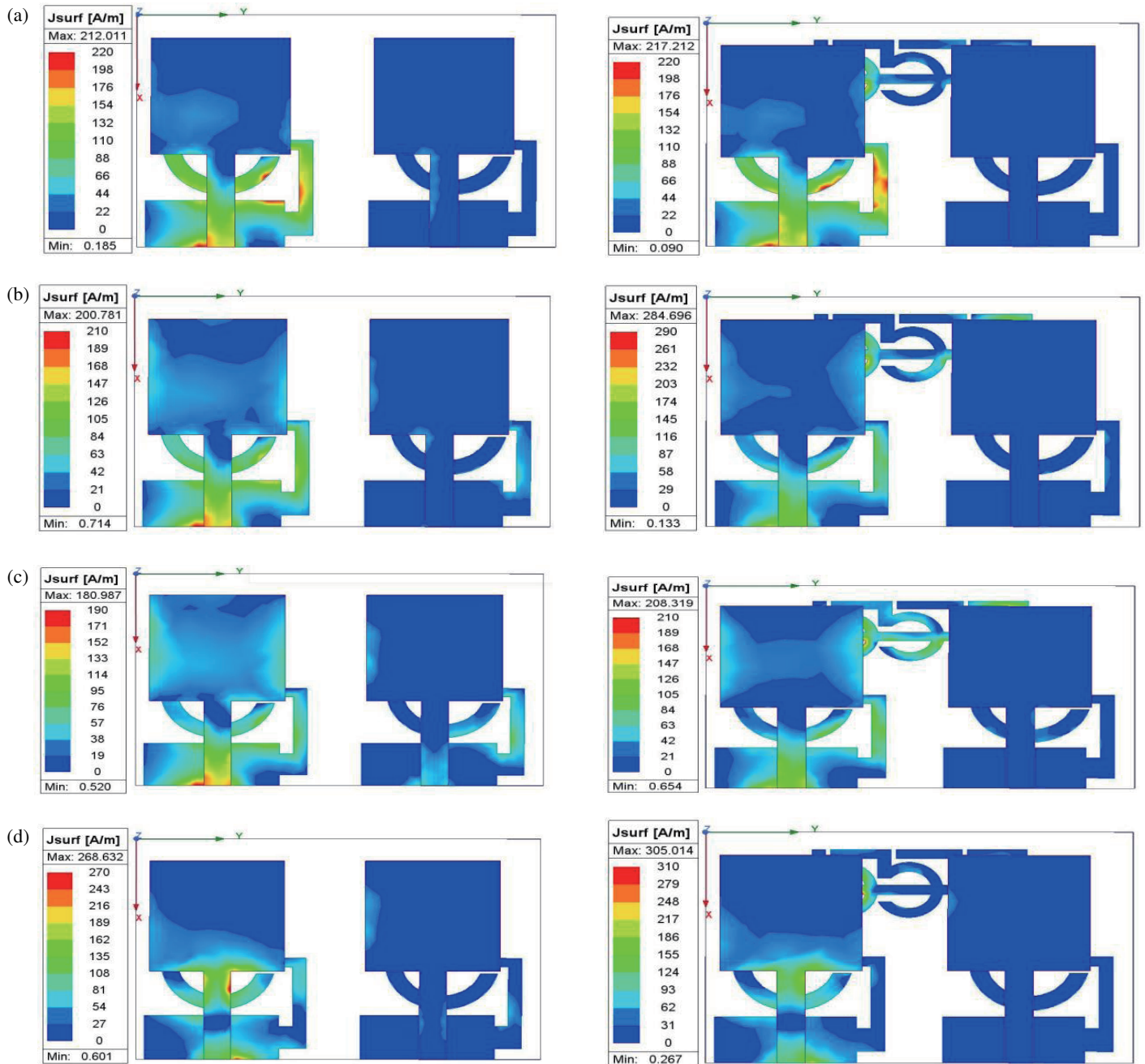


**FIGURE 5.** (a)  $S$ -parameters variation with decoupling element, surface current distribution of MIMO antenna (a) at 11.54 GHz, (b) 12.26 GHz, (c) 13 GHz and (d) 17.28 GHz.

over 80% across its operational frequency range, with a maximum gain of 5.54 dB at 16.37 GHz, as indicated in Figure 6(c).

The antenna's performance is further assessed through the examination of diversity parameters [20]. The diversity parameters, such as Envelope Correlation Coefficient (ECC), are computed using the  $S$ -parameters as shown in Equation (6). The ECC value for the operational band is below the threshold of 0.1, specifically less than 0.05. This proposed antenna demonstrates excellent performance parameters, making it very suitable for acceptance. The simulated and measured values of ECC and DG (Diversity Gain) are shown graphically in Fig-

ure 6(d).

$$ECC = \frac{|S_{11}^* S_{12} + S_{21}^* S_{22}|^2}{(1 - |S_{11}|^2 - |S_{21}|^2)(1 - |S_{22}|^2 - |S_{12}|^2)} \quad (6)$$

$$DG = 10\sqrt{1 - ECC^2} \quad (7)$$

$$TARC = \sqrt{\frac{(S_{11} + S_{12})^2 + (S_{22} + S_{21})^2}{2}} \quad (8)$$

$$C_{LOSS} = -\log_2 |\varphi^R| \quad (9)$$

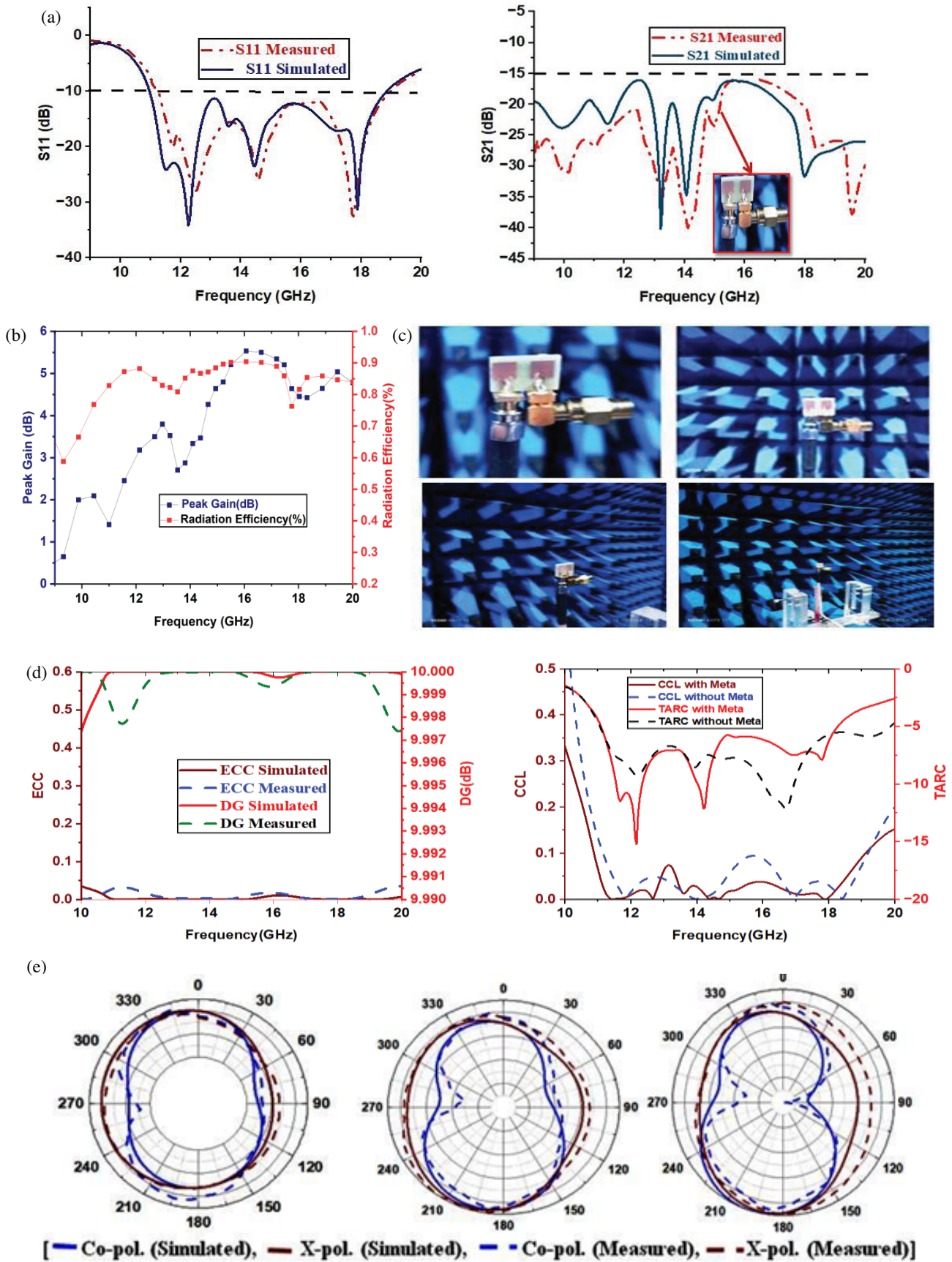


**FIGURE 6.** S-parameter Variation with simulated and measured antenna, (a)  $S_{11}$  &  $S_{21}$ , (b) Peak gain vs Radiation efficiency, (c) Prototype of fabricated antenna, (d) ECC vs DG and CCL Vs TARC and (e) Radiation pattern at 12.12 GHz, 15.5 GHz and 16.06 GHz.

**TABLE 3.** Parametric analysis of proposed work with existing works.

| Ref. No         | Array Elements | Dimensions (mm <sup>2</sup> ) | Decoupling Technique                     | Operating band            | Isolation (dB)     | ECC              |
|-----------------|----------------|-------------------------------|--|---------------------------|--------------------|------------------|
| [21]            | 2 × 2          | 37 × 70                       | EMBG based on metamaterial               | X, Ku, K & Ka             | < -15 dB           | < 0.1            |
| [3]             | 2 × 2          | 48 × 35                       | 5SRR                                     | 2–18 GHz                  | < -20 dB           | < 0.1            |
| [22]            | 2 × 2          | 15 × 25                       | Metamaterial                             | X & Ku                    | < 20 dB            | < 0.1            |
| [23]            | 2 × 2          | 20 × 30                       | Metasurfacesquare wave slot pattern      | X, Ku, K & Ka             | < -15 dB           | < 0.1            |
| [15]            | 2 × 2          | 23 × 23                       | EBG based metamaterial                   | X, Ku, K & Ka             | < -15 dB           | < 0.05           |
| [13]            | 2 × 2          | 62.75 × 0.75                  | Metasurface                              | X, Ku & K bands           | < -20 dB           | < 0.1            |
| [16]            | 2 × 2          | 22.5 × 14                     | SNG metamaterial                         | 3.08–14.1                 | < -15 dB           | < 0.06           |
| [14]            | 2 × 2          | 60 × 60                       | Metasurface                              | 3.1–6.2, 7.1–8.7          | < -15 dB           | < 0.07           |
| [4]             | 2 × 2          | 45 × 25                       | CSRR metasurfaces                        | 4.42–4.87 & 8.11–8.98 GHz | < -20 dB           | < 0.05           |
| <b>Proposed</b> | <b>2 × 2</b>   | <b>10 × 15</b>                | <b>3 Single SRR based Tank Structure</b> | <b>10.97 to 18.85 GHz</b> | <b>&lt; -16 dB</b> | <b>&lt; 0.05</b> |

Additional parameters, such as total active reflection coefficient (TARC) as below 12 dB, channel capacity losses (CCL) as 0.2 bits/sec/Hz within band covering from 10.97 to 18.85 GHz, DG at 9.98 dB, are also computed using Equations (7), (8) & (9) shown in Figure 6(d).

#### 4.1. Comparison of Proposed Work With Previous Works

The proposed design is significantly smaller and more compact, with a miniaturization of 75% than the references [4, 15, 16, 22, 23], specifically [23]. Bandwidth and isolation are enhanced in comparison to the references [15, 23]. According to the data in Table 3, the MIMO antenna that was proposed achieved excellent performance across multiple parameters, indicating its suitability for a wide range of applications.

## 5. CONCLUSION

A compact wideband MIMO antenna incorporating a three single-SRR based tank metastructure has been designed, fabricated, and tested. The implementation of a ground tank circuit and three single-SRR metastructures, placed between the antenna elements at the base of MIMO systems, results in effective isolation and minimal channel losses, measuring below 0.2 bits/sec/Hz. The proposed MIMO antenna operates in the frequency band of 10.97 GHz to 18.85 GHz. It achieves an isolation of over 16 dB, with a maximum of -31.32 dB at 17.88 GHz. This frequency range encompasses the higher end of the X-band and Ku-band. The proposed antenna is extremely versatile due to its compact size and low profile, enabling it to function effectively in wide band applications while maintain-

ing good isolation. The system incorporates a novel single-SRR tank circuit for decoupling, with diversity parameters including ECC less than 0.05 and DG as 9.98 dB. The MIMO system achieves radiation efficiency and miniaturization rates of over 80% and 75%, respectively. This work explores the potential of radar applications in a wide operating range, demonstrating good isolation and the ability to achieve multiple operating bands by increasing the number of array elements in the design.

## ACKNOWLEDGEMENT

The Department of ECE at IIIT Naya Raipur provides help for antenna measuring test facilities. The authors express their gratitude to the HOD and everyone in the Department of ECE at the Indian Institute of Information Technology (IIIT) Raipur.

## REFERENCES

- [1] Sakli, H., C. Abdelhamid, C. Essid, and N. Sakli, "Metamaterial-based antenna performance enhancement for MIMO system applications," *IEEE Access*, Vol. 9, 38 546–38 556, 2021.
- [2] Garg, P. and P. Jain, "Isolation improvement of MIMO antenna using a novel flower shaped metamaterial absorber at 5.5 GHz WiMAX band," *IEEE Transactions on Circuits and Systems II: Express Briefs*, Vol. 67, No. 4, 675–679, 2020.
- [3] Sakli, H., C. Abdelhamid, C. Essid, and N. Sakli, "Metamaterial-based antenna performance enhancement for MIMO system applications," *IEEE Access*, Vol. 9, 38 546–38 556, 2021.
- [4] Armghan, A., S. K. Patel, S. Lavadiya, S. Qamar, M. Alsharari, M. G. Daher, A. A. Althuwayb, F. Alenezi, and K. Aliqab, "Design and fabrication of compact, multiband, high gain, high isolation, metamaterial-based MIMO antennas for wireless communication systems," *Micromachines*, Vol. 14, No. 2, 357, 2023.

- [5] Wang, Z., L. Zhao, Y. Cai, S. Zheng, and Y. Yin, "A meta-surface antenna array decoupling (MAAD) method for mutual coupling reduction in a MIMO antenna system," *Scientific Reports*, Vol. 8, No. 1, 3152, 2018.
- [6] Wang, Z., C. Li, Q. Wu, and Y. Yin, "A metasurface-based low-profile array decoupling technology to enhance isolation in MIMO antenna systems," *IEEE Access*, Vol. 8, 125 565–125 575, 2020.
- [7] Xue, C.-D., X. Y. Zhang, Y. F. Cao, Z. Hou, and C. F. Ding, "MIMO antenna using hybrid electric and magnetic coupling for isolation enhancement," *IEEE Transactions on Antennas and Propagation*, Vol. 65, No. 10, 5162–5170, 2017.
- [8] Deng, J., J. Li, L. Zhao, and L. Guo, "A dual-band inverted-F MIMO antenna with enhanced isolation for WLAN applications," *IEEE Antennas and Wireless Propagation Letters*, Vol. 16, 2270–2273, 2017.
- [9] Zhu, J., S. Li, S. Liao, and Q. Xue, "Wideband low-profile highly isolated MIMO antenna with artificial magnetic conductor," *IEEE Antennas and Wireless Propagation Letters*, Vol. 17, No. 3, 458–462, 2018.
- [10] Ramachandran, A., S. V. Pushpakaran, M. Pezholil, and V. Kesavath, "A four-port MIMO antenna using concentric square-ring patches loaded with CSRR for high isolation," *IEEE Antennas and Wireless Propagation Letters*, Vol. 15, 1196–1199, 2015.
- [11] Tan, X., W. Wang, Y. Wu, Y. Liu, and A. A. Kishk, "Enhancing isolation in dual-band meander-line multiple antenna by employing split EBG structure," *IEEE Transactions on Antennas and Propagation*, Vol. 67, No. 4, 2769–2774, 2019.
- [12] Govindarajulu, S. R., A. Jenkel, R. Hokayem, and E. A. Alwan, "Mutual coupling suppression in antenna arrays using meandered open stub filtering technique," *IEEE Open Journal of Antennas and Propagation*, Vol. 1, 379–386, 2020.
- [13] Khan, M. S., A.-D. Capobianco, M. F. Shafique, B. Ijaz, A. Naqvi, and B. D. Braaten, "Isolation enhancement of a wideband mimo antenna using floating parasitic elements," *Microwave and Optical Technology Letters*, Vol. 57, No. 7, 1677–1682, 2015.
- [14] Pan, B. C. and T. J. Cui, "Broadband decoupling network for dual-band microstrip patch antennas," *IEEE Transactions on Antennas and Propagation*, Vol. 65, No. 10, 5595–5598, Oct. 2017.
- [15] Zhang, S., B. K. Lau, Y. Tan, Z. Ying, and S. He, "Mutual coupling reduction of two PIFAs with a T-shape slot impedance transformer for MIMO mobile terminals," *IEEE Transactions on Antennas and Propagation*, Vol. 60, No. 3, 1521–1531, Mar. 2012.
- [16] Zhai, G., Z. N. Chen, and X. Qing, "Enhanced isolation of a closely spaced four-element MIMO antenna system using metamaterial mushroom," *IEEE Transactions on Antennas and Propagation*, Vol. 63, No. 8, 3362–3370, Aug. 2015.
- [17] Li, H., B. K. Lau, Z. Ying, and S. He, "Decoupling of multiple antennas in terminals with chassis excitation using polarization diversity, angle diversity and current control," *IEEE Transactions on Antennas and Propagation*, Vol. 60, No. 12, 5947–5957, Dec. 2012.
- [18] Alibakhshikenari, M., B. S. Virdee, I. C. H. See, R. Abd-Alhameed, F. Falcone, A. Andujar, J. Anguera, and E. Limiti, "Study on antenna mutual coupling suppression using integrated metasurface isolator for SAR and MIMO applications," in *2018 48th European Microwave Conference (EuMC)*, 1425–1428, 2018.
- [19] Alibakhshikenari, M., M. Khalily, B. S. Virdee, C. H. See, R. A. Abd-Alhameed, and E. Limiti, "Mutual-coupling isolation using embedded metamaterial EM bandgap decoupling slab for densely packed array antennas," *IEEE Access*, Vol. 7, 51 827–51 840, 2019.
- [20] Alibakhshikenari, M., M. Khalily, B. S. Virdee, C. H. See, R. A. Abd-Alhameed, and E. Limiti, "Mutual coupling suppression between two closely placed microstrip patches using EM-bandgap metamaterial fractal loading," *IEEE Access*, Vol. 7, 23 606–23 614, 2019.
- [21] Undrakonda, J. and R. K. Upadhyayula, "Isolation analysis of miniaturized metamaterial-based MIMO antenna for X-band radar applications using machine learning model," *Progress In Electromagnetics Research C*, Vol. 124, 135–153, 2022.
- [22] Alibakhshikenari, M., B. S. Virdee, I. C. H. See, R. Abd-Alhameed, F. Falcone, A. Andujar, J. Anguera, and E. Limiti, "Study on antenna mutual coupling suppression using integrated metasurface isolator for SAR and MIMO applications," in *2018 48th European Microwave Conference (EuMC)*, 1425–1428, 2018.